Analytical Evaluation of Fitted Piston Compression Ring: Modal Behaviour and Frictional Assessment

Christopher Edward Baker, Homer Rahnejat, Ramin Rahmani and Stephanos Theodossiades

Loughborough University

ABSTRACT

Piston compression rings are thin, incomplete circular structures which are subject to complex motions during a typical 4-stroke internal combustion engine cycle. Ring dynamics comprises its inertial motion relative to the piston, within the confine of its seating groove. There are also elastodynamic modes, such as the ring in-plane motions. A number of modes can be excited, dependent on the net applied force. The latter includes the ring tension and cylinder pressure loading, both of which act outwards on the ring and conform it to the cylinder bore. There is also the radial inward force as the result of ring-bore conjunctional pressure (i.e. contact force). Under transient conditions, the inward and outward forces do not equilibrate, resulting in the small inertial radial motion of the ring. The conjunctional friction, comprising viscous shear of the lubricant and any boundary friction as the result of direct interaction of surfaces also act on the ring, as well as the inertial force in the axial direction of the cylinder. Therefore, ring motions are quite complex. However, with properly fitted rings, the radial modal behaviour of the ring is the most important. This provides an opportunity to determine the *in-situ* ring shape analytically by assuming a series of quasi-static steps in which the balance between ring tension and pressure induced forces with the instantaneous contact force is assumed.

The resulting ring shape yields the ring-bore gap, allowing the determination of frictional losses for a given bore out-of-roundness and surface topography. A subsequent analysis based upon one dimensional lubricated conjunction for certain ring configurations enables evaluation of lubricant flow and any chance of oil loss and blow-by. This fully analytical as opposed to computationally intensive numerical analysis is verified with FEA.

INTRODUCTION

The power losses in internal combustion engines can be divided into two key categories; thermodynamic and parasitic. Thermodynamic losses include those due to heat, for example, heat expelled from the exhaust and heat losses from surfaces through conduction or convection. These losses account for 50-60% of the total engine losses. Parasitic losses such as friction or due to pumping account for 25%. These inefficiencies mean that only approximately 15% of the input power is available to propel the vehicle, overcoming road friction and any aerodynamic drag. Of the 25% lost due to friction, almost half is lost within the piston mechanism. A quarter is down to engine bearings, whilst around 10-15% is through valve train frictional forces. The remainder is accounted for with the sum of small inefficiencies within the system. Compression rings can be seen to be responsible for 4-5% of all losses in a standard 4-stroke internal combustion engine (Mishra *et al*, 2009). Clearly this is a significant proportion of all losses, especially for such a relatively small component. In order to reduce the frictional losses due to the compression ring, a comprehensive model is first required to understand all aspects of the forces and motions encountered.

Previous studies on the tribology of piston ring cylinder liner conjunction have treated the compression ring as a rigid body, with no global deformation (modal behaviour). However due to the forces applied, particularly at the firing crank angle in the engine, intuition alone suggests that both in-plane and out-of-plane deflections of the compression ring from its original shape should take place. This can in turn affect the conformability of piston ring to the cylinder liner. The latter itself is subject to global deformations due to dynamic loadings, thermal distortion and initial (static) deformations originated from manufacturing and machining processes.

In fact, the conformability of piston ring to cylinder liner has long been the subject of interest for engine designers. Any gap between the ring and liner can be a source of excessive oil consumption and increased blow-by. This gap can be caused by factors such as the bore out-of-roundness, limitations in ring's elastic behaviour and distortion of cylinder liner due to thermal and mechanical (vibrational) loads and in-plane and out of plane vibrations of piston ring. The problem has been addressed by some researchers. In one of the earlier studies Loenne and Ziemba (1989) measured the cylinder bore distortions using an 'Incometer'. They found that a typical cylinder can hold various orders of distortion. The second order distortion of a cylinder refers to its ovality, whilst the third and fourth orders arise from machining and excessive tightening of the cylinder head bolts, respectively (Bardzimashvili *et al*, 2005). Hill and Newman (1985) introduced the concept of 'ring conformability factor' in order to quantify the ability of a ring to seal a given bore distortion. Using an empirical relationship, they were able to describe the radial deformation for a cylinder at given order which can be sealed by a ring with a known conformability factor. Later, Dunaevsky (1990) and Dunaevsky *et al* (2000, 2002 and 2005) expanded the ring-bore conformability analysis and introduced a rigorous mathematical method to model the conformability of a ring to a distorted bore profile. They also studied the conformability of the rings with non-symmetrical cross-sections (Dunaevsky and Alexandrov 2005). A semi-empirical relation to determine the maximum bore deformation that a ring can conform to has also been introduced by Tomanik (1996) and Mueller (2005). Bardzimashvili *et al* (2004) examined various existing conformability criteria with a ring-pack model and concluded that the higher orders of deformations may need to be considered as well as the effect of gas pressure. A summary of the existing empirical and/or analytical methods is given in Dunaevsky and Rudzitis (2007).

Ma *et al* (1997) implemented the ring bore gap calculation into their tribological model. They used Hill and Newman's method and also incorporated the gas force effect. They showed that gas force can aid conformation of the ring with a distorted bore profile, especially at and near TDC. All the studies cited thus far ignore ring modal behaviour subjected to a transient force balance.

Early studies of ring dynamics took the form of analyzing curved bars. Lamb (1888) was among the first to perform this analysis. He discussed the in-plane flexure of a uniform bar. Based on the previous work by Kirchoff, Clebsch, Thomson and Tait, a general equation for free-free end conditions was derived and solved. However, Lamb's work only considered beams with a small curvature. Den Hartog (1927) built on this work by deriving formulae for the first and second natural frequencies of an incomplete circular ring. He applied the Rayleigh-Ritz energy method to obtain the natural frequencies for both hinged and clamped boundary conditions. Brown (1934) presented an approximate solution for the out-of-plane vibrations problem, using a modification to the Rayleigh method. He found that the calculated values using this method were higher than those obtained through experimentation. However, these fell within the level of expected error. Later Volterra and Morell (1961) used the Rayleigh-Ritz method to find the lowest natural frequencies for various elastic arcs, in and out-of-plane of curvature. Further to this, they applied the theory to elastic hinged arcs.

Love (1944) obtained the classical equation of motion for an incomplete ring of small cross-section. He assumed an undeformed central radial axis in order to evaluate the global deformation of an incomplete circular ring. He obtained various modal frequencies using a previous work attributed to Mayer. The ring was considered with different types of applied normal loads. Archer (1960) studied the in-plane in-extensional vibrations of incomplete rings with small cross-sections. The results were obtained using classical equations of motion, considering only in-plane forces. The results found by Archer for rings of angular extension between π and 2π were in agreement with den Hartog's results. Shear deformation was neglected in his studies. However, Timoshenko (1955) proved that this was a valid assumption. Lang (1962) found solution forms for both extensional and in-extensional deformation theories regarding thin circular rings. He considered both the modal response and forced excitation.

The current study aims to show the importance of including ring-bore conformability in tribological assessment of piston ring-to-cylinder liner conjunction. In addition, deformation of a given ring under load is investigated in order to provide a first step towards the inclusion of inertial ring dynamics in tribological studies.

RING BORE CONFORMABILITY

A typical engine cylinder profile was measured using a coordinate measuring machine (CMM). To be able to measure the cylinder a block consisting of two cylinders was cut-off from a V8 engine (see Figure 1). This *in-situ* liner has already been subject to thermal and mechanical loads, as well as embodying the usual initial manufacturing imperfections and post-processing (such as honing) effects. The measurements provide the real shape of the bore at any given cross-section.
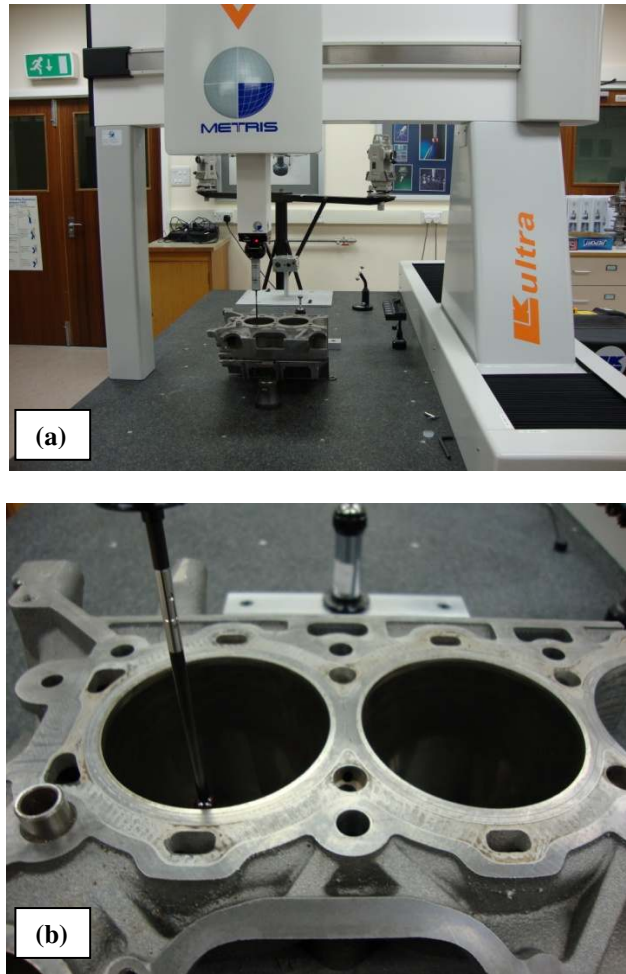
Figure 1 – (a) The CMM arrangement and (b) the measured block sample

The cylinder profile was measured at several axial heights. The heights at which the measurements were taken are shown in Figure 2. These represent the deviation of the measured liner profile from a nominal (average) radius. In these measurements the top dead centre (TDC) was considered as the reference position. The second cross-section corresponds to the location where maximum combustion pressure occurs in the power stroke. A typical combustion gas pressure curve is shown in Figure 3. Study of this point is of further importance as the combustion gas force (Hill and Newman, 1985) is one of the main contributors to the cylinder liner deformation.
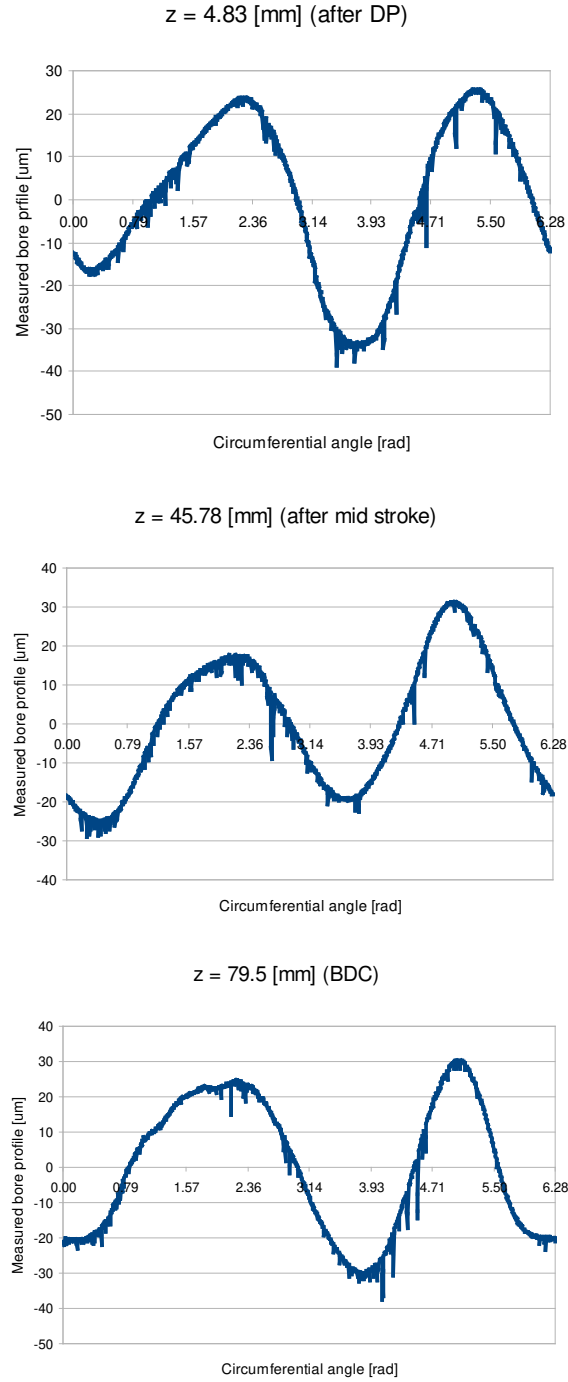
z = 4.83 [mm] (after DP)

z = 45.78 [mm] (after mid stroke)

z = 79.5 [mm] (BDC)
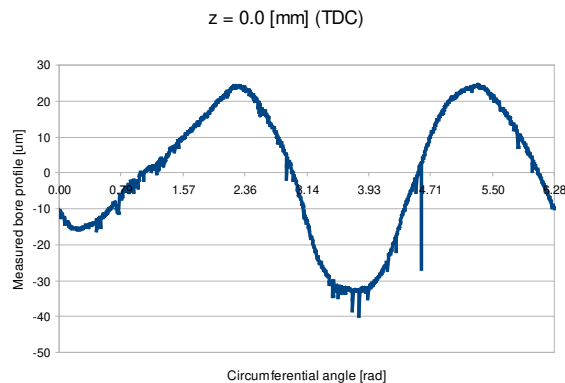
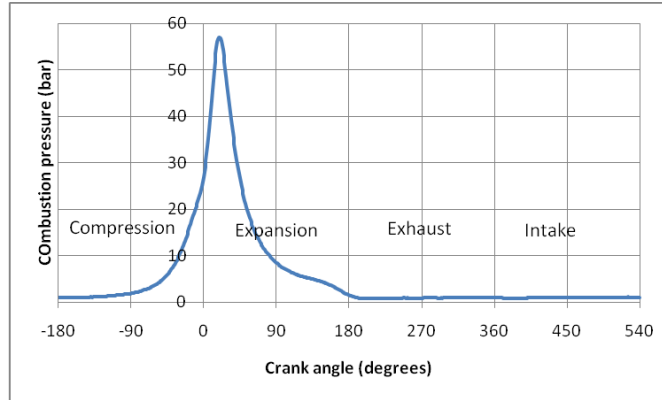*Figure 2 – Measured cylinder profile at various axial cross-sections*

Figure 3 – Variations of combustion gas pressure with the crank angle at 2000rpm

The measured shape of the liner can be described using a Fourier series:

$$\zeta(\theta) = r + \sum_{k=1}^{n} [A_k \cos(k\theta) + B_k \sin(k\theta)]$$

(1)

where *r* is the average (nominal) bore radius. The maximum distortion of any order (any term of the series) can then be calculated from the Fourier coefficients as:

$$U_k = \left(A_k^2 + B_k^2\right)^{\frac{1}{2}}$$

(2)

Given a ring with known characteristics and associated loading, one needs to obtain a relationship for ring-liner conformance. Various analytical and/or (semi-) empirical relations can be used. In this study, the conformability criteria given by Mueller, Tomanik, Dunaevsky, and Hill and Newman are studied (see Introduction). Table 1 compares these four conformability analyses as described by Bardzimashvili, *et al* (2005) and Newman and Hill (1985).

Table 1 – Various relations for critical deformations

Mueller (1970)	$\dfrac{Kr}{(n^2 - 1)^2}$
Dunaevsky (1990)	$\dfrac{Kr}{3(n^2 - 1)}$
Tomanik (1996)	$\dfrac{Kr}{20(n^2 - 1)}$
Hill and Newman (1985)	$\dfrac{Kr}{4(n^2 - 1)^2}$

The parameter *K* in Table 1 is called the ring conformability coefficient (or factor) and is defined as:

$$K = \frac{F_T r^2}{E I_r}$$

(3)

in which F_T is the tangential force which is required to close the ring gap and r is the nominal bore radius.

In the case of Hill and Newman (1985) conformability relation, this factor is expressed as:

$$K = \frac{F_T (2r - d)^2}{EI_r}$$

(4)

where d is radial thickness of the ring.

Each point on a ring having an initial end gap of γ, after being fitted to a circular cylinder with a nominal radius of r would have a radial deformation which can be described by the following equation (Bin Chik and Fessler, 1966):

$$u(\theta) = Kr\left(1 + \cos\theta + \frac{\pi - \theta}{2}\sin\theta\right)$$

(5)

The uniform elastic pressure exerted by the ring can also be found as:

$$P_e = \frac{\gamma EI}{3\pi br^4}$$

(6)

Therefore, the tangential force of the ring can be obtained as:

$$F_T = P_e br$$

(7)

Using the equation above one can obtain the deformed ring profile from its free state with an initial end gap. Figure 4 shows the resulted deformed ring profile for the compression ring studied in the current work.
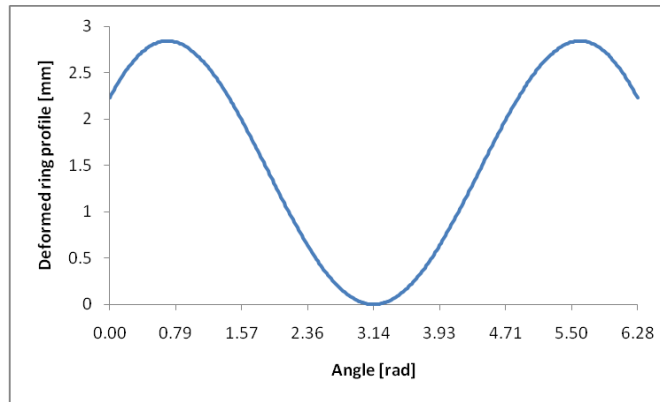

Figure 4 – The predicted deformation in the ring profile after being fitted to a circular bore of nominal diameter

The applied force in these relations takes into account only the ring tension force. However, in an engine other forces also arise. The most prominent force is the combustion gas force, which is assumed to act on the ring back face. This force is expected to enhance ring-bore conformability. This effective gas force is added to the ring tension force, yielding the total outward force on the ring as:

$$F = F_T + P_g br$$

(8)

in which P_g is the gas pressure (Figure 3) and b is the ring axial face-width.

Figure 5 represents the ring bore gap which is obtained using the Tomanik's bound with the total applied force F. A gap appears with the 4th order of bore distortion ($n = 4$). Dunaevsky's analytical method predicts no gap even for relatively high bore orders. Thus, the ring bore gap can be examined based on the other methods listed in Table 1 (Figure 6).
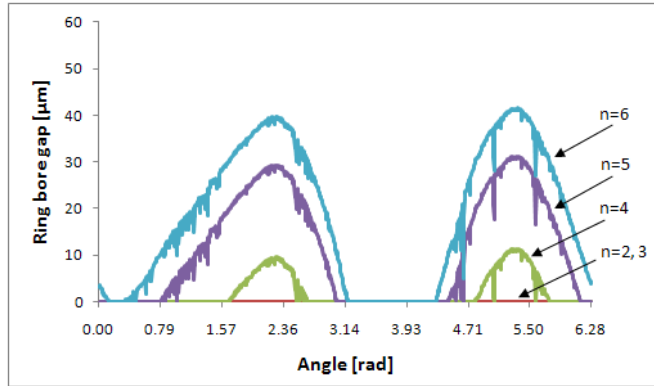

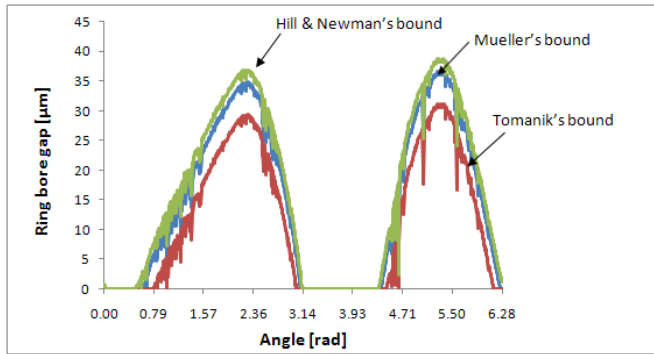*Figure 5 – Studied ring bore gap based on Tomanik's bound*

Figure 6 – A comparison of obtained ring bore gap using different criteria

It can be seen that the gap predicted using the Tomanik's bound is the lowest of all for a bore distorted dominantly by an order of five.

TRIBOLOGICAL ANALYSIS

In order to investigate the effect of ring bore gap on the tribological performance of the engine, a two-dimensional computer model to solve the lubrication problem, using Reynolds' equation under quasi-static condition (radial force balance) is used. A parabolic axial ring profile was assumed for a worn compression ring. Isothermal conditions were assumed for this initial analysis, eliminating the effect of viscous shear heating of the lubricant. The surface roughness parameters used in Greenwood and Tripp (1971) were measured for the given liner surface. The ring tension and gas loading represent the contact force under quasi-static conditions. This force is sustained by hydrodynamic lubricant reaction and by the asperity interactions.

The bore cross section at which Reynolds' equation was solved was selected to be that corresponding to the point after the maximum combustion pressure. The data used are given in Table 2.

Table 2 – Data for the tribological study

Parameter	Value

Engine stroke	79.5 mm
Engine speed	2000 rpm
Bore nominal radius	44.52 mm
Modulus of elasticity of ring	203 GPa
Ring face-width	1.2 mm
Liner surface roughness (RMS)	0.26 µm
Lubricant density	849.7 kg/m^3 @ 15 [°C] 833.8 kg/m^3 @ 40 [°C]
Lubricant kinematic viscosity	59.99 cSt @ 40 [°C] 9.590 cSt @ 100 [°C]

The result of the analysis yields the minimum clearance as shown in Figure 7. As expected, the conformability obtained using the Hill and Newman's bounds resulted in the lowest minimum clearance, which yields the worst case scenario. However, it must be noted that these predictions for the ring bore gap change for the other orders of distortion. The dominant order of distortion for the bore is obtained using the Fourier analyses as shown by equation (1) and calculating the maximum amplitude of deformations through subsequent DFT or FFT analyses.
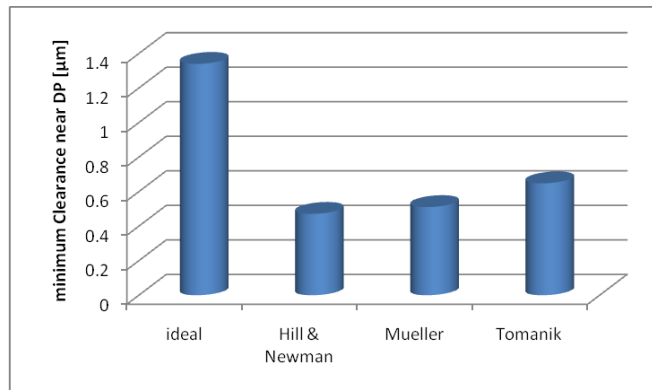

Figure 7 – Predicted minimum clearance with different conformability criterion

Figure 8 compares the predicted minimum film thicknesses for a complete engine cycle for an ideal circular bore with a distorted bore as described above, based on the bounds obtained using Mueller's method. It is assumed that the predicted gap between the ring and the bore at the studied point (DP) is more or less prevalent at other cross-sections as well. This is reasonable, given the measured profiles at different cross sections shown in Figure 2. The results show that the difference can be significant when the gas pressure is low. At these points, the sealing ability of the ring is compromised. Zero degrees crank angle represents the TDC position in power stroke.
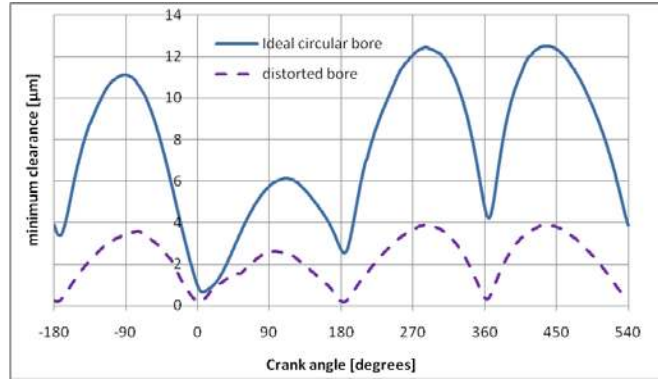
Figure 8 – Minimum conjunctional gap for ideal and distorted bores

Hitherto, these analyses ignore the ring dynamics. In fact, the ring bore conjunction can be affected by ring dynamics, which should be taken into account at any crank angle position during the engine cycle.

DYNAMICS OF THE PISTON RING: NATURAL FREQUENCIES AND MODE SHAPES

Figure 9 shows the in-plane motion degrees of freedom for an incomplete circular ring, with a radius significantly larger than its face-width (thin structure).
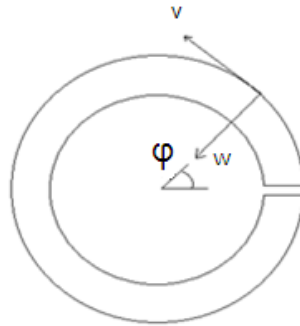

Figure 9 – Incomplete ring, in-plane motion degrees of freedom, as used by Lang (1962)

By neglecting rotary inertia, and considering the radial and tangential forces, as well as bending moments, the equations of motion for radial and tangential displacements are:

$$\frac{\partial^5 v}{\partial \varphi^5} + 2\frac{\partial^3 v}{\partial \varphi^3} + \frac{\partial v}{\partial \varphi} + \frac{1}{\rho \omega^2}\frac{\partial^3 v}{\partial \varphi \partial t^2} - \frac{1}{\rho \omega^2}\frac{\partial^4 v}{\partial t^2} =$$

$$\frac{a^3}{EI}\left\{\frac{\partial}{\partial \varphi}\left[F_R(\varphi,t)\right] - F_T(\varphi,t)\right\}$$

(9)

$$\frac{\partial^6 w}{\partial \varphi^6} + 2\frac{\partial^4 w}{\partial \varphi^4} + \frac{\partial^2 w}{\partial \varphi^2} + \frac{1}{\rho \omega^2}\frac{\partial^4 w}{\partial \varphi^2 \partial t^2} - \frac{1}{\rho \omega^2}\frac{\partial^4 w}{\partial t^2} =$$
$$\frac{a^3}{EI}\left\{\frac{\partial}{\partial \varphi}\left[F_R(\varphi, t)\right] - F_T(\varphi, t)\right\}$$

(10)

Both equations need to be separated as performed by Archer (1960), into space and time expressions. This gives three solution forms for v and w, where the appropriate solution is determined by the nature of λ value in:

$$\sigma_n^6 + 2\sigma_n^4 + (1 - \lambda_n)\sigma_n^2 + \lambda_n = 0$$

(11)

Letting $\xi = \sigma^2$:

$$\xi_n^3 + 2\xi_n^2 + (1 - \lambda_n)\xi_n + \lambda_n = 0$$

(12)

Equation (12) is the characteristic equation of the eigenproblem, a cubic expression in σ^2. Depending on the value of λ a number of solutions exist according to Lang. Those applicable to inextensional deformation of an incomplete ring, yield:

For: $0.113401 < \lambda^2 < 17.6366$, $\xi_{n1} = \pm id_n$, $\xi_{n2} = \delta_n \pm i\mu$ and $\xi_{n3} = -\delta_n \pm i\mu$.

And for: $\lambda^2 > 17.6366$, $\xi_{n1} = -d_n^2$, $\xi_{n2} = e_n^2$, $\xi_{n3} = f_n^2$.

The modal response equations are in the form:

$$V_n = f(\varphi, \xi_{ni}), W_n = g(\varphi, \xi_{ni}), \qquad j = 1,2,3,\cdots$$

(13)

Evaluation of these equations of motion gives the natural frequencies of the ring, and the resulting mode shapes at each modal frequency, f_n:

$$f_n = \frac{1}{2\pi}\sqrt{\frac{\lambda EI}{mR^4}}$$

(14)

DYNAMICS OF THE PISTON RING: FORCED RESPONSE OF AN INCOMPLETE RING

Equations (9) and (10), as stated previously, are partial differential equations. Whilst the space-based response solves the natural frequencies and mode shapes as described above, the time-based response is also required for a full solution, so that:

$$v(\varphi, t) = \sum_{n=1}^{\infty} V_n(\varphi)\eta(t)$$

(15)

For the dynamic response of the system:

$$\eta_n + \omega_n^2 \eta_n = Q(t)$$

(16)

Where

$$Q_n(t) = -\frac{\int_0^\alpha V_n \left\{ \frac{\partial}{\partial \varphi} F_R(\varphi, t) - F_T(\varphi, t) \right\} d\varphi}{\rho a A \int_0^\alpha (W_n^2 + V_n^2) d\varphi}$$

(17)

F_R and F_T are the radial and tangential force components, respectively. The solution to equation (16) takes the form:

$$\eta_n(t) = \frac{1}{\omega_n} \int_0^t Q_n(\tau) \sin \omega_n(t - \tau) d\tau + C_{n1} \sin \omega_n t + C_{n2} \cos \omega_n t$$

(18)

Where C_{n1} and C_{n2} are constants dependent on the initial displacement and velocity conditions:

$$C_{n1} = \frac{\int_0^\alpha (\dot{v_0} V_n + \dot{w_0} W_n) d\varphi}{\omega_n \int_0^\alpha (W_n^2 + V_n^2) d\varphi}, \quad C_{n2} = \frac{\int_0^\alpha (v_0 V_n + w_0 W_n) d\varphi}{\int_0^\alpha (W_n^2 + V_n^2) d\varphi}$$

(19)

Hence equation (15) provides the full space-time solution.

In addition, the elastic force acting on the ring comes from equations (6) and (7) above. The gas pressure acting on the ring is regarded as constant circumferentially.

DYNAMICS OF THE PISTON RING: CASE STUDY

The method for calculating the natural frequencies was verified through FEA for a free incomplete ring. Snapshots of the mode shapes were compared with the analytical solution. Table 3 shows the values of the parameter used in this ring model.

Table 3 – Values used in calculation of natural frequencies and mode shapes

Elastic modulus, E	210 GPa
Density, ρ	7800 kg/m^3
Ring thickness, d	3.5mm
Axial width, w	1.198mm
Nominal ring radius, R	43mm
Second moment of area, I_r	4.2e-12 m^4
Ring angle, α	359°

Figure 10 shows an example mode shape taken from the FEA analysis. This is for comparison with Figure 11, which shows the shape obtained by implementing Lang's analytical method. The mode number is $n = 8$.
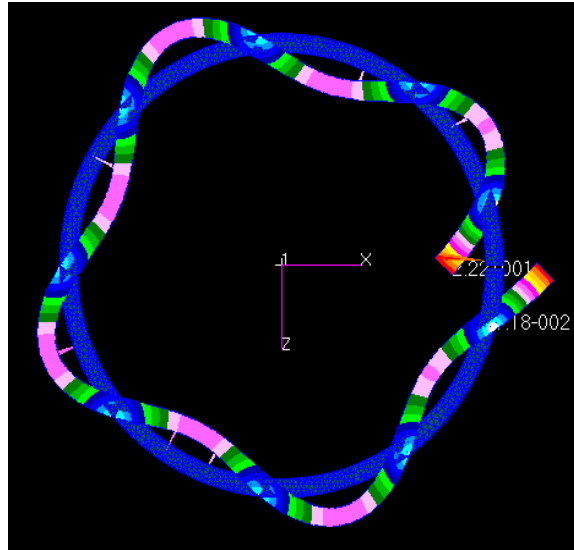
Figure 10 – Snapshot of the FEA mode shape when f = 7457Hz
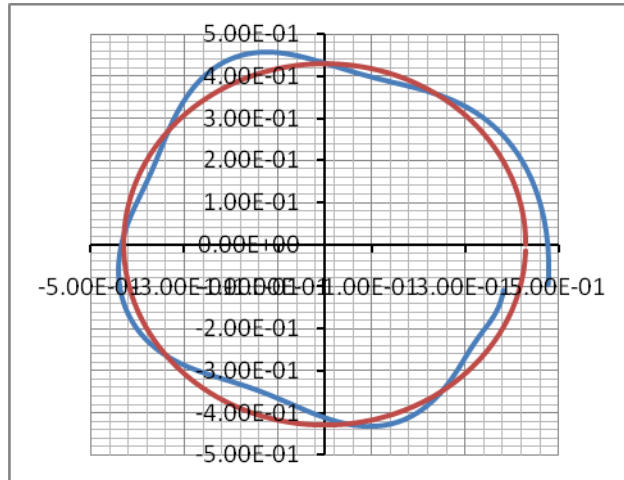
Figure 11 – Plotted mode shape for f = 7363Hz

Table 4 gives a comparison of all the FEA results with the calculated natural frequencies.

Table 4 – Natural frequency values from FEA and Lang's method

Lang (Hz)	FEA (Hz)	% difference
151.96	198.31	23.37
383.9	432.35	11.21
1350	969.76	28.15
1895.1	1795.4	5.26
2533.4	2871.9	11.79
3924	4181.7	6.16
5532	5712.8	3.16
7363	7457	1.26

SUMMARY/CONCLUSIONS

This study shows the importance of including some salient practical features in tribological studies of compression ring-bore/liner conjunction, which are often neglected in literature. One is bore out-of-roundness; the other is conformance of the ring to such a bore, both in fitment and with applied gas pressure. Furthermore, the elastodynamic behaviour of an *in-situ* ring is important as under transient conditions the net force acting on the ring alters. The inclusion of all these features makes for computationally intensive analysis, which is mitigated by closed form analytical solutions for ring dynamics and analytical or semi-empirical representation of ring-bore conformance. At the same time this level of detail and beyond is required in order to reliably estimate the conjunctional gap, with the view to estimate regime of lubrication and most importantly evaluate friction. The ultimate aim of any analysis should be to predict friction and oil losses. The balance between these two key requirements is the essence of ring function. Further required detail is implied here, because another key function of the compression ring is to conduct the heat away from the conjunction, often forming a very thin film of lubricant. For this purpose simultaneous solution of energy equation with Reynolds' equation is necessary, as well as adjusting for lubricant viscosity. These represent the immediate future extensions of this research.

REFERENCES

Archer, R. R. (1960), Small Vibrations of Thin Incomplete Circular Rings, Int. J. Mech. Sci., Vol. 1, pp. 45-56

Bardzimashvili, T., Kelly, J.F., Romelashvili, E. (2004), Distortion inside a Piston Bore, 2004, URL (last accessed: 24/10/10)
http://www.math.msu.edu/Academic_Programs/graduate/msim/MSIMProjectReports/piston0428.pdf

Bardzimashvili, T., Kelly, J.F., Romelashvili, H., Sledd, W.T., Geist, B. (2005), A Multiple Order Conformability Model for Uniform Cross-Section Piston Rings, SAE paper 2005-01-1643

Bin Chik, A., Fessler, H. (1966), Radial pressure exerted by piston rings, Journal of Strain Analysis, Vol. I, No. 2, pp. 165-171

Brown, F. H. (1934), Lateral Vibration of Ring Shaped Frames, J. Franklin Inst., Vol. 217, pp. 41-48

Den Hartog, J. P. (1928), The Lowest Natural Frequency of Circular Arcs, Philos. Mag., Vol. 5, No. 7, pp 400-408

Dunaevsky, V.V. (1990), Analysis of Distortions of Cylinders and Conformability of Piston Rings, Tribology Transactions, Vol. 3, No. 1, pp. 33-40

Dunaevsky, V., Alexandrov, S., Barlat, F. (2000), Analysis of Three-Dimensional Distortions of the Piston Rings with Arbitrary Cross-Section, SAE paper 2000-01-3453

Dunaevsky, V., Alexandrov, S. (2002), Development of Conformability Model of Piston Rings with Consideration of Their Three-Dimensional Torsional Distortions and Fourier Series Representation of Cylinder Bore Geometry, SAE paper 2002-01-3131

Dunaevsky, V., Alexandrov, S. (2005), Three-Dimensional Engineering Approach to Conformability Analysis of Piston Rings, Tribology Transactions, Vol. 48, No. 1, pp. 108-118

Dunaevsky, V., Rudzitis, J. (2007), Clarification of a Semi-Empirical Approach in Piston Ring-Cylinder Bore Conformability Prediction, ASME Journal of Tribology, Vol. 129, pp. 430-435

Greenwood, J.A., Tripp, J.H. (1970-71), The Contact of Two nominally Flat Rough Surfaces, Proc. Instn. Mech. Engrs., Vol. 185, pp. 625-633

Hill, S.H., Newman, B.A. (1985), Piston Ring Designs for Reduced Friction, SAE paper 841222

Lamb, H. (1888), On the Flexure and Vibrations of a Curved Bar, Proc. Lond. Math. Soc., Vol. 19, pp 365-376

Lang, T. E. (1962), Vibration of Thin Circular Rings, Part 1, Jet Propulsion Laboratory Technical Report No. 32-261

Loenne, K., Ziemba, R. (1989), The GOETZE Cylinder Distortion Measurement System and the Possibility of Reducing Cylinder Distortions, SAE paper 880142

Love, A. E. H., A Treatise on Mathematical Theory of Elasticity, 1944, Dover, NewYork

Ma, M.-T., Smith, E.H., Sherrington, I. (1977), Analysis of Lubrication and Friction for a Complete Piston-Ring Pack with an Improved Oil Availability Model, Part 2: Circumferentially Variable Film, Proc. Instn. Mech. Engrs., Part J, Vol. 21, pp. 17-27

Mishra, P.C., Balakrishnan, S., Rahnejat, H. (2008), Tribology of the Compression Ring-to-Cylinder Contact at Reversal, Proc. IMechE Part J: J. Mech. Eng. Sci., Vol. 222, pp. 815-826

Mishra, P.C., Rahnejat, H., King, P.D. (2009), Tribology of the Ring-Bore Conjunction Subject to a Mixed Regime of Lubrication, Proc. IMechE Part C: J. Mech. Eng. Sci., Vol. 223, pp. 987-998

Timoshenko, S., Goodier, J.N., Theory of Elasticity, 2nd Ed., 1951, McGraw-Hill, Inc., US

Tomanik, E. (1996), Piston Ring Conformability in a Distorted Bore, SAE paper 960356

Volterra, E., Morell, J. D. (1961), Lowest Natural Frequency of Elastic Arc for Vibrations outside the Plane of Initial Curvature, ASME J. App. Mech., Vol. 28, pp. 624-627

CONTACT INFORMATION

Wolfson School of Mechanical and Manufacturing Engineering,

Loughborough University,

Loughborough,

Leicestershire LE11 3TU

UK

Tel: +44 (1509) 227686

Fax: +44 (1509) 227648

Email: C.E.Baker@lboro.ac.uk

ACKNOWLEDGMENTS

NOMENCLATURE

A_k, B_k Fourier coefficients

b, h ring face width (axial height)

C_{n1}, C_{n2}	Dynamic response constants
d	radial thickness of ring
d_n	Root parameter
E	Young elasticity modulus
F	total force
F_R, F_T	excitation forces (radial and tangential)
f	frequency of vibration
I_r	Second moment of area of ring
K_n	conformability factor
k	summation index
m	mass per unit area of ring
n	order of deformation, mode number
P_e	elastic pressure
P_g	gas pressure
Q	generalised force term
R	nominal ring radius
r	nominal bore radius
r_i	inner radius of ring
r_o	outer radius of ring
t	time
U_n	maximum bore deformation
u	ring deformation
v, w	displacement (tangential and radial)
V_n, W_n	modal function, (tangential and radial)

Greek symbols

α	subtended angle of ring

γ	ring end gap
δ, μ	root parameters
ζ	deviation from average
θ	circumferential angle
λ	frequency parameter
ξ	σ^2
ρ	density of ring material
σ	root
φ	crank angle
ω	frequency of vibration

Abbreviations

2D	two-dimensional
CMM	Coordinate Measuring Machine
DFT	Discrete Fourier Transform
DP	Detonation Point
FEA	Finite Element Analysis
FFT	Fast Fourier Transform
RMS	Root Mean Square
rpm	Revolution per minute
TDC	Top Dead Centre